



GMAO RESEARCH BRIEF

June 2020

Transition to the RRTMG Shortwave Radiation Code in GEOS Models

Peter Norris, Lawrence L. Takacs, William Putman, Lawrence Coy, Steven Pawson (GSFC/GMAO), Eli Mlawer, Michael Iacono (AER, Inc.)

SUMMARY

In January 2020, the GMAO introduced the shortwave component (SW) of the radiative transfer module RRTM for global climate model (GCM) applications (RRTMG; Iacono et al., 2008) into the GEOS-FP (forward processing) analysis and prediction system. This inclusion completes the long-term plan to transition from the Chou-Suarez to the RRTMG radiation codes. RRTMG is an efficient, actively maintained, modern and flexible code base better adapted for future model development.

The initial implementation of RRTMG_SW, in GEOS-5.25p3, resulted in a cold bias in stratospheric temperatures when compared to both independent observations and the previous GEOS-FP system (GEOS-5.22). Adjustments introduced in GEOS-5.25p5 resulted in improved radiative heating rates in the 200-263nm spectral band, primarily impacted by ozone and oxygen heating in the stratosphere and lower mesosphere. This upgrade substantially improved the analyzed and predicted temperatures in the stratosphere of the GEOS-FP system and GEOS-5.25p5 became the production system in April 2020.

BACKGROUND

Radiative transfer is one of the most important atmospheric processes. This report summarizes the changes made to the solar-heating code in Version 5.25 of the GEOS Model. The Chou-Suarez heating code used in prior versions of GEOS-5 has been replaced by the RRTMG solar heating modules as part of the GMAO's endeavor to upgrade the entire suite of physical parameterizations in the model. This report describes how problems encountered during development and implementation were resolved.

Introduction

The NASA Global Modeling and Assimilation Office (GMAO) is transitioning the Global Earth Observing System (GEOS) model to include contemporary representations of all processes with code bases designed to run efficiently on modern high-performance computing platforms. This includes a transition from the long-standing Chou-Suarez radiation parameterizations (Chou and Suarez, 1999; Chou et al., 2001) to the more modern, flexible RRTM for GCM applications (RRTMG) parameterizations (Iacono et al., 2008). RRTMG parameterizations are expected to be faster for more vertical levels and to have continued community support. The RRTMG longwave (LW) code was implemented in GEOS-FP with the upgrade to GEOS-5.21 in July 2018. The RRTMG shortwave (SW) code was introduced into GEOS-FP with the transition to GEOS-5.25p3 in January 2020 and updated with the adoption of GEOS-5.25p5 in April 2020. Other changes introduced with the GEOS-5.25 systems include upgrades to the Catchment land-surface modules (Koster et al., 2020) and new representations of clouds and turbulence.

The RRTMG Radiation Code

The stand-alone RRTM code is developed and maintained by Atmospheric and Environmental Research Inc. (AER) (Clough et al., 2005; Mlawer et al., 1997). RRTM utilizes the correlated k-distribution approach to accurately and efficiently calculate fluxes and heating rates. It uses g-point absorption and extinction coefficient interpolation tables derived directly from AER's line-by-line radiative transfer model (LBLRTM) with up-to-date and validated spectroscopy (e.g., Clough et al., 2005; Alvarado et al., 2013; Mlawer et al. 2019). In the LW (10-3250 cm^{-1}), RRTM uses 16 spectral bands with 16 g-points in each band; in the SW (820-50000 cm^{-1}) it uses 14 such bands. This amounts to 256 monochromatic calculations in the LW and 224 in the SW. The flux accuracy of RRTM compared with LBLRTM is $\lesssim 1.5 \text{ W/m}^2$ in LW and $\lesssim 1 \text{ W/m}^2$ (direct) and $\lesssim 2 \text{ W/m}^2$ (diffuse) in the SW. The LW molecular absorbers are water vapor, carbon dioxide, ozone, nitrous oxide, methane, oxygen, nitrogen, and halocarbons. The SW sources of extinction are water vapor, carbon dioxide, ozone, nitrous oxide, methane, oxygen, aerosols, and Rayleigh scattering. The Chou-Suarez SW parameterization does not include nitrous oxide and methane heating.

The GCM version of RRTM, named RRTMG, reduces the number of g-points to 140 and 112 in the LW and SW, respectively, to improve efficiency with minimal impact on accuracy. The LW flux accuracy compared with LBLRTM is $\lesssim 1.5 \text{ W/m}^2$; the SW flux

accuracy compared RRTM is $\lesssim 3 \text{ W/m}^2$. Accuracy is improved in some spectral bands in the LW code by replacing the standard diffusivity angle (secant 1.66) used for angular integration with a diffusivity angle that varies with total column water vapor. The SW code uses a two-stream algorithm to perform scattering calculations. For gas optics, the essence of the correlated k-distribution method is interpolation of the absorption coefficients for each g-point to the GCM layer temperature and pressure using large look-up-tables derived from the LBL calculations. In bands where there is a mixture of two major absorbing gases with overlapping spectra, the code uses an additional interpolation dimension based on the ratio of concentrations of the two gases.

RRTMG uses the McICA (Monte-Carlo Independent Column Approximation; Pincus et al., 2003) to integrate over sub-grid-column optical variability. Cloud properties can vary greatly at the unresolved sub-grid-column scale of a GCM, and the radiative effect of clouds is strongly non-linear. A common way to estimate the grid-scale mean radiative effect is to generate a set of statistically representative “sub-columns,” or pixels, consisting of binary clear/cloudy sub-grid cells with homogeneous properties. However, running the full radiation parameterization on each sub-column is prohibitively expensive. The McICA method employed by RRTMG distributes the sub-columns randomly among the many g-points, effectively absorbing the subcolumn dimension cost into the spectral integration but adding statistically unbiased noise over the spatial and temporal sampling provided by a dynamical model.

The cloud overlap assumptions used by Chou-Suarez and RRTMG also differ. Chou-Suarez uses a cloud-fraction-only overlap with maximum overlap in low-, middle-, and high-pressure bands and random overlap between them. RRTMG uses the considerably more sophisticated “generalized” (exponential) overlap scheme of Räisänen et al. (2004), which includes exponential decorrelation in both cloud mask and condensate. The particular implementation, which includes latitude and seasonal variations in decorrelation length scales, is discussed in depth in Oreopoulos and Norris (2011) and Oreopoulos et al. (2012).

In addition, the RRTMG SW code includes a parameterization of the NRLSSI2 (Naval Research Laboratory Solar Spectral Irradiance) model (Lean and Woods, 2010) for solar input. This includes secular and spectral solar variability from sunspot dimming and facular brightening.

The RRTMG in GEOS Models

The RRTMG LW code was adopted in GEOS-5.21, which became the production version of GEOS-FP in July 2018. The RRTMG SW code was introduced into GEOS-FP in January 2020, when GEOS-5.25p3 replaced GEOS-5.22p2 as the production system. GMAO's testing and validation of the RRTMG SW code initially revealed a cold bias in stratospheric temperatures compared to the Chou-Suarez SW code. However, given the GMAO's strategic pathway for model developments, this was not regarded as an obstacle to making the change because the impact of the cold bias was outweighed by computation benefits and improvements in tropospheric performance. Figure 1 shows the zonal-mean SW heating rates in GEOS-5.25p3 are smaller than in GEOS-5.22p2 for December 2019. The differences (Fig. 1c) highlight the weaker solar heating in the newer system, with heating rate differences peaking at about -2 K/day near the summer polar stratopause (1 hPa near 90°S) and a modest additional warming peaking near 3 hPa. The differences decrease further away from the summer pole, where the solar insolation is the largest, and disappear near the terminator where there is no solar heating in December.

Following reports of a similar cold bias in the European Centre for Medium Range Weather Forecasts (ECMWF) model, AER suggested tuning the variable `LAYREFFR` in the shortest UV band (band 28, 200-263 nm) of RRTMG SW from its original value (58) to values around 40. This variable can be understood in the context of the correlated k-distribution method of RRTMG:

- The k-distribution method uses LBL-precalculated absorption tables $k_g(\ln p, T, \eta)$ for each wavenumber band and each g-point in the band. Here η relates to the ratio between the concentrations of the two major absorbers, which for band 28 are O_3 and O_2 . The actual absorption coefficient for each model grid-box is obtained by trilinear interpolation into these tables.
- RRTMG also requires specification of the input solar energy, S_g , into each g-point for the model grid-column as a whole. However, the split of S between g-points depends on the mix η of O_3 and O_2 , which varies by *layer*. Hence, one representative model layer is chosen to determine η and then S_g by linear interpolation into a pre-calculated $S_g(\eta)$ table. That representative layer is the model layer with pressure near `pref(LAYREFFR)`, where `pref` is the RRTMG table of reference pressures.

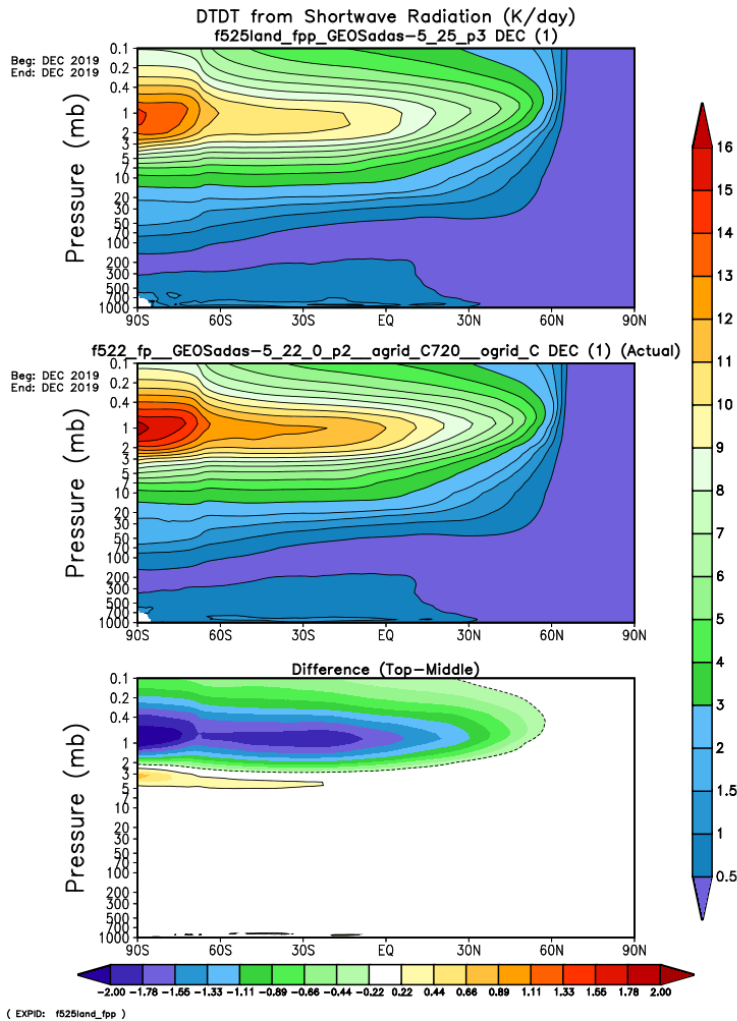


Figure 1. Zonal-mean SW heating rates (K/day) in December 2019 for the candidate replacement system (GEOS-5.25p3, top), the GEOS-FP system (GEOS-5.22p2, middle) and their difference (newer minus older systems, bottom).

The problem with the original `LAYREFFR` value of 58 is that it corresponds to a level at the GEOS model top (0.01 hPa), well above the predominant layer of absorption in band 28. Choosing a `LAYREFFR` somewhere near 1 hPa, where the dominant absorption in this band is occurring, is more physically meaningful. The `pref` values for our GMAO test cases, with `LAYREFFR` of 35, 40, and 45, correspond to pressures of about 1.17, 0.43, and 0.16 hPa, respectively. All three test cases improved the SW heating rate profile significantly from the original `LAYREFFR` of 58, but the value 40 produced the greatest overall improvement.

[Ultimately it's not `pref(LAYREFFR)` that matters, but the O_3/O_2 mix associated with that pressure. So, if η does not vary much around 1 hPa, a big difference between different `LAYREFFR` will not be seen around that pressure. It should also be noted that only one `pref(LAYREFFR)` for band 28 of RRTMG can be selected. If that pressure varied significantly with season, it might be necessary to specify a seasonal cycle for `LAYREFFR`. In fact, the very small seasonal variation in the peak absorption height in this band does not warrant this.]

Concurrent with the GMAO tests, AER conducted its own study and released a new RRTMG SW version v4.10, with a tuned band 28 `LAYREFFR` of 42. This updated RRTMG release also fixed a minor issue related to the consistent treatment of Rayleigh scattering between RRTMG and the line-by-line code LBLRTM that determines its absorption coefficient tables. Therefore, RRTMG SW v4.10 was adopted in GEOS-5.25p4, where it reduced the shortwave heating bias to approximately -0.4 K/day with respect to the MERRA-2 reanalysis (Fig. 2). These improved heating rates are also in much closer agreement with those from the Chou-Suarez code used in earlier GEOS model versions.

As further demonstration of the benefits of the updated RRTMG SW v4.10, Fig. 3 shows the analyses and forecasts of 1 hPa Southern Hemisphere Extratropical temperature made using GEOS-5.25p3 and GEOS-5.25p4. The clear drift toward colder temperatures over the five-day forecast duration using the original RRTMG SW version (Fig. 3a) is substantially reduced with the updated version (v4.10; Fig. 3b), and the 1 hPa temperature in the analyses is several tenths of a degree warmer when the updated RRTMG SW code is used.

Transition to the RRTMG Shortwave Radiation Code in GEOS Models

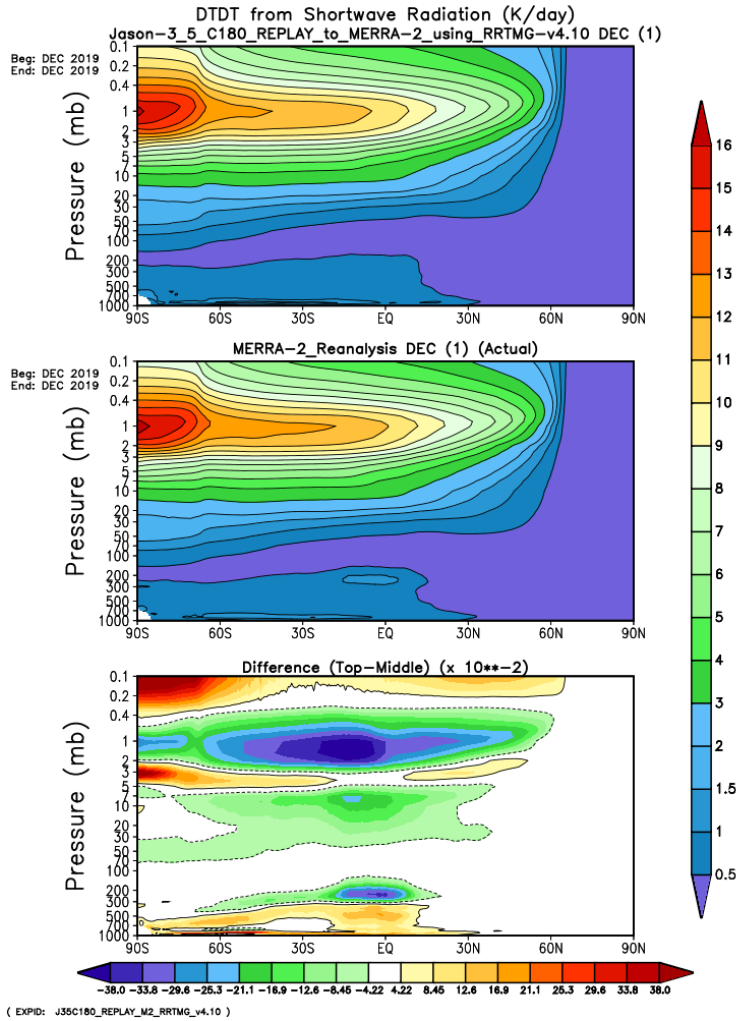


Figure 2. Zonal-mean SW heating rates (K/day) in December 2019 for the updated RRTMG system (GEOS-5.25p4, top), the MERRA-2 reanalysis system (GEOS-5.17, middle), and the difference (bottom). Note that the differences in solar heating rates are plotted in hundredths of one K/day in this plot, while in Fig. 1 they are plotted in K/day.

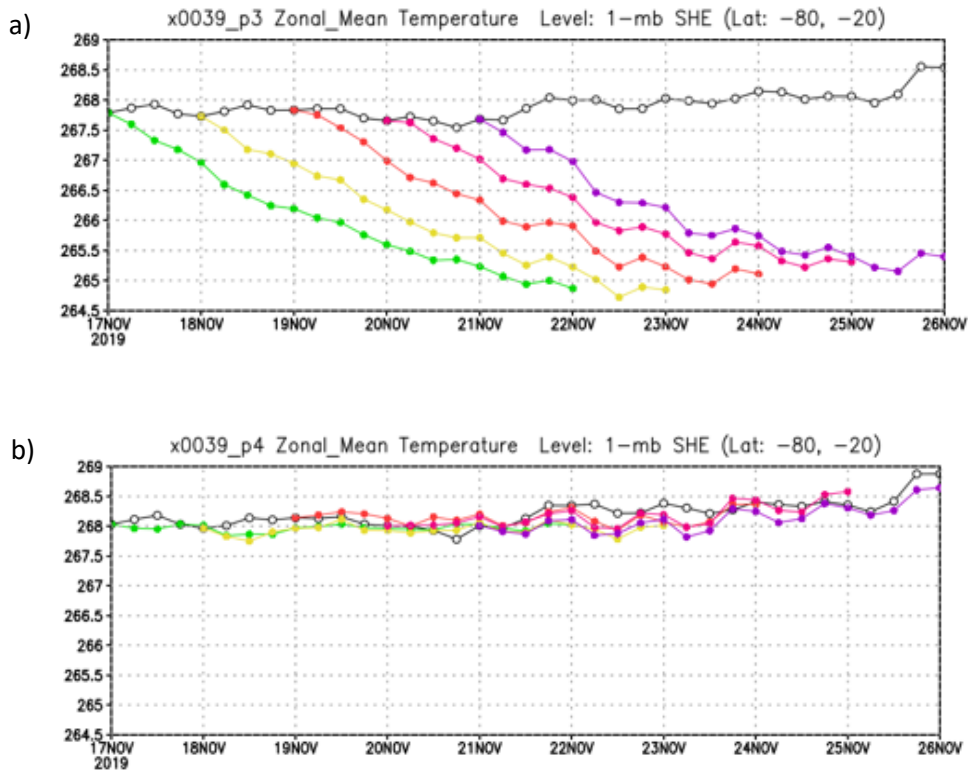


Figure 3. Time series of southern hemispheric (80°-20°S) temperature at 1 hPa in the GEOS analyses, shown every six hours, and in daily five-day forecasts using GEOS-5.25p3 (top) and GEOS-5.25p4 (bottom). The top plot is the GEOS-FP version introduced in January 2020 and the bottom plot uses the same RRTMG SW version as the replacement GEOS-FP introduced in April 2020.

Summary and Future Work

The original implementation of RRTMG SW in the GEOS-FP (Version 5.25p3) led to a large decrease in radiative heating rates in the upper stratosphere, when compared with earlier GEOS systems that use the Chou-Suarez solar code (e.g., Version 5.22p2). The decreased heating rates resulted in GEOS analyses having a colder stratopause than in earlier GEOS-FP systems. Forecasts using GEOS-5.25p3 showed a rapid cooling of several degrees over five days, leading to large cold biases in forecast temperatures (Fig. 3). Retuning of the 200-263nm spectral interval in RRTMG SW substantially reduced the low bias in solar heating rates. Implementation of Version 4.10 of RRTMG SW into GEOS-5.25p4 and p5 reduced the observed heating rate bias, which in turn led to analyzed temperatures in the upper stratosphere agreeing more closely with those in earlier GEOS versions and eliminated the rapid drift in forecast temperatures in the upper stratosphere.

The updates introduced into GEOS-5.25p4 were combined with other changes (to the convection parametrization) in GEOS-5.25p5. GEOS-5.25p5 replaced GEOS-5.25p3 as the GMAO's GEOS-FP production system in April 2020.

An additional difference between the Chou-Suarez and RRTMG SW codes is that while RRTMG does not consider wavelengths lower than 200nm, the Chou-Suarez code extends down to 175nm. The small amount of missing solar energy in the 175-200nm range ($\sim 0.08 \text{ W m}^{-2}$) could account for less heating in the Schumann Runge bands of molecular oxygen in GEOS-5.25 than in GEOS-5.22. This absorption peaks much higher in the atmosphere (around 100 km) and has negligible effect ($< 0.1 \text{ K/day}$) around 1 hPa. Spectral variations in solar output at these short wavelengths are, however, known to be important for determining ozone variations and solar heating rates in the mesosphere and may be needed for some GEOS-based studies of upper stratospheric processes. AER is currently working on adding a band to RRTMG SW that will extend below 200 nm to include this UV oxygen absorption and other processes relevant to the upper stratosphere and lower mesosphere. GMAO expects to implement these changes when they are released.

References

Alvarado, M. J., V.H. Payne, E.J. Mlawer, G. Uymin, M.W. Shephard, K.E. Cady-Pereira, J.S. Delamere, and J.-L. Moncet, 2013: Performance of the Line-By-Line Radiative Transfer Model (LBLRTM) for temperature, water vapor, and trace gas retrievals: recent updates evaluated with IASI case studies. *Atmos. Chem. Phys.*, **13**, 6687-6711, doi:10.5194/acp-13-6687-2013.

Chou, M.-D., and M. Suarez, 1999: A Solar Radiation Parameterization for Atmospheric Studies. *Technical Report Series on Global Modeling and Data Assimilation 104606*, Vol. 15. <https://gmao.gsfc.nasa.gov/pubs/docs/Chou136.pdf> (1880 kB).

Chou, M.-D., M. Suarez, X.-Z. Liang, and M. M.-H. Yan, 2001: A Thermal Infrared Radiation Parameterization for Atmospheric Studies. *Technical Report Series on Global Modeling and Data Assimilation 104606*, Vol. 19. <https://gmao.gsfc.nasa.gov/pubs/docs/Chou137.pdf> (1954 kB).

Clough, S.A. and M.J. Iacono, 1995: Line-by-line calculation of atmospheric fluxes and cooling rates: 2. Application to carbon dioxide, ozone, methane, nitrous oxide and the halocarbons. *J. Geophys. Res.-Atmos.*, **100**, 16519-16535, <https://doi.org/10.1029/95JD01386>.

Clough, S.A., M.W. Shephard, E.J. Mlawer, J.S. Delamere, M.J. Iacono, K. Cady-Pereira, S. Boukabara and P.D. Brown, 2005: Atmospheric radiative transfer modeling: a summary of the AER codes. *J. Quant. Spectrosc. Radiat. Transfer*, **91**, 233-244.

Iacono, M.J., J.S. Delamere, E.J. Mlawer, M.W. Shephard, S.A. Clough, and W.D. Collins, 2008: Radiative forcing by long-lived greenhouse gases: Calculations with the AER radiative transfer models. *J. Geophys. Res.*, **113**, D13103, doi:10.1029/2008JD009944.

Lean, J. and T. N. Woods, 2010: Solar spectral irradiance measurements and models, *Evolving Solar Physics and the Climates of Earth and Space*, K. Schrijver and G. Siscoe Eds., Cambridge University Press, 269-298.

Koster et al., 2020: Land Focused Changes in the Updated GEOS-FP System (Version 5.25). GMAO Research Brief (March 2020), available at https://gmao.gsfc.nasa.gov/researchbriefs/land_changes_GEOS-FP/land_changes_GEOS-FP.pdf

Mlawer, E.J., S.J. Taubman, P.D. Brown, M.J. Iacono, and S.A. Clough, 1997: Radiative transfer for inhomogeneous atmospheres: RRTM, a validated correlated-k model for the longwave, *J. Geophys. Res.*, **102**, 16,663-16,682.

Mlawer, E. J., D. D. Turner, S. N. Paine, L. Palchetti, G. Bianchini, V. H. Payne, K. E. Cady-Pereira, R. L. Pernak, M. J. Alvarado, D. Gombos, J. S. Delamere, M. G. Mlynczak, and J. C. Mast, 2019: Analysis of water vapor absorption in the far-infrared and submillimeter regions using surface radiometric measurements from extremely dry locations, *J. Geophys. Res.*, **124**, 8134-8160, doi:10.1029/2018JD029508.

Oreopoulos, L. and P.M. Norris, 2011: An analysis of cloud overlap at a midlatitude atmospheric observation facility. *Atmos. Chem. Phys.*, **11**, 5557-5567.

Oreopoulos L., D. Lee, Y.C. Sud, and M.J. Suarez, 2012: Radiative impacts of cloud heterogeneity and overlap in an atmospheric General Circulation Model. *Atmos. Chem. Phys.*, **12**, 9097-9111, doi:10.5194/acp-12-9097-2012.

Pincus, R., H.W. Barker, and J.-J. Morcrette, 2003: A fast, flexible, approximate technique for computing radiative transfer in inhomogeneous clouds. *J. Geophys. Res.*, **108(D)**, 4376, doi:10.1029/2002JD003322.

Räisänen P., H.W. Barker, M.F. Khairoutdinov, J. Li, D.A. Randall, 2004: Stochastic generation of subgrid-scale cloudy columns for largescale models. *Q. J. R. Meteorol. Soc.*, **130**, 2047-2068.